

Farnesoid X Receptor and its ligands inhibit the function of platelets

Article

Accepted Version

Figures and Legends

Moraes, L. A., Unsworth, A. J., Vaiyapuri, S. ORCID: <https://orcid.org/0000-0002-6006-6517>, Ali, M. S., Sasikumar, P., Sage, T., Flora, G. D., Bye, A. P. ORCID: <https://orcid.org/0000-0002-2061-2253>, Kriek, N., Dorchies, E., Molendi-Coste, O., Dombrowicz, D., Staels, B., Bishop-Bailey, D. and Gibbins, J. M. ORCID: <https://orcid.org/0000-0002-0372-5352> (2016) Farnesoid X Receptor and its ligands inhibit the function of platelets. *Arteriosclerosis Thrombosis and Vascular Biology*, 36 (12). pp. 2324-2333. ISSN 1524-4636 doi: <https://doi.org/10.1161/ATVBAHA.116.308093> Available at <https://centaur.reading.ac.uk/67335/>

It is advisable to refer to the publisher's version if you intend to cite from the work. See [Guidance on citing](#).

To link to this article DOI: <http://dx.doi.org/10.1161/ATVBAHA.116.308093>

Publisher: Lippincott, Williams & Wilkins

All outputs in CentAUR are protected by Intellectual Property Rights law, including copyright law. Copyright and IPR is retained by the creators or other copyright holders. Terms and conditions for use of this material are defined in the [End User Agreement](#).

www.reading.ac.uk/centaur

CentAUR

Central Archive at the University of Reading

Reading's research outputs online

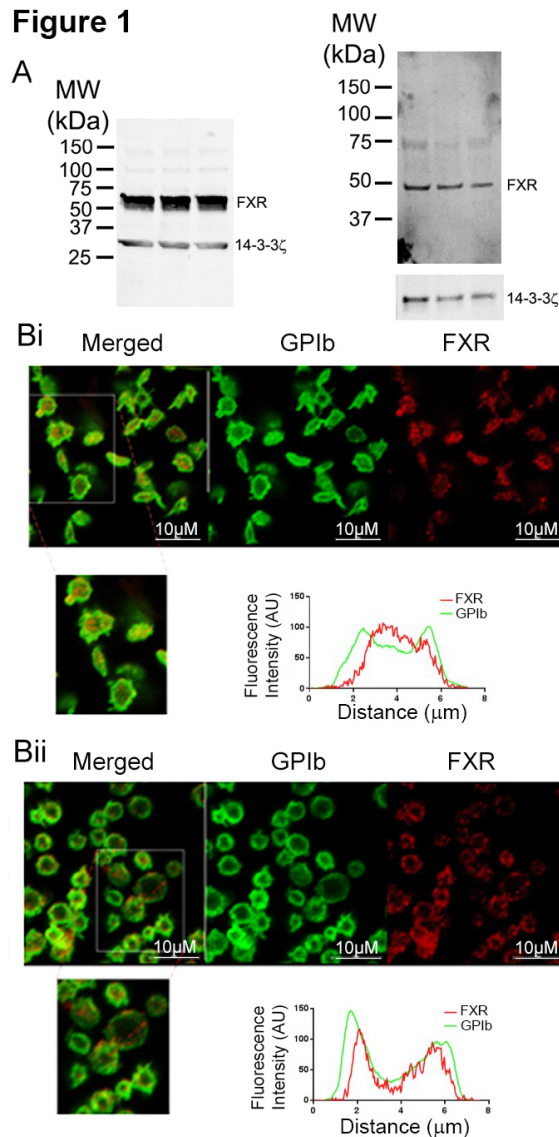


Figure 1 – FXR is expressed in human and mouse platelets. (A) Whole human and mouse platelet lysates, samples from 3 separate donors or mice, were immunoblotted (IB) to detect FXR. The localization of FXR in human platelets was analysed by immunofluorescence confocal microscopy. (B) Unstimulated (i) and stimulated (using U46619 (20μM) in the presence of Integrilin (4μM)) platelets (ii) in PRP were fixed in 4% (v/v) paraformaldehyde-PBS. Platelets were permeabilised (in the presence of 0.2% triton X-100, donkey serum and 1% PBS-BSA) and stained for FXR (in red) and GPIb (in green). Visualisation of cells was performed using a Nikon A1-R confocal microscope and 100x oil immersion lens. In resting and activated platelets, FXR was found to be dispersed throughout the platelet volume in a punctate arrangement. Line plot analysis was performed across resting and stimulated platelets that also indicated partial re-localisation of FXR towards the plasma membrane following activation. The data for line plots are representative of >7 cells (representative data shown).

Figure 2

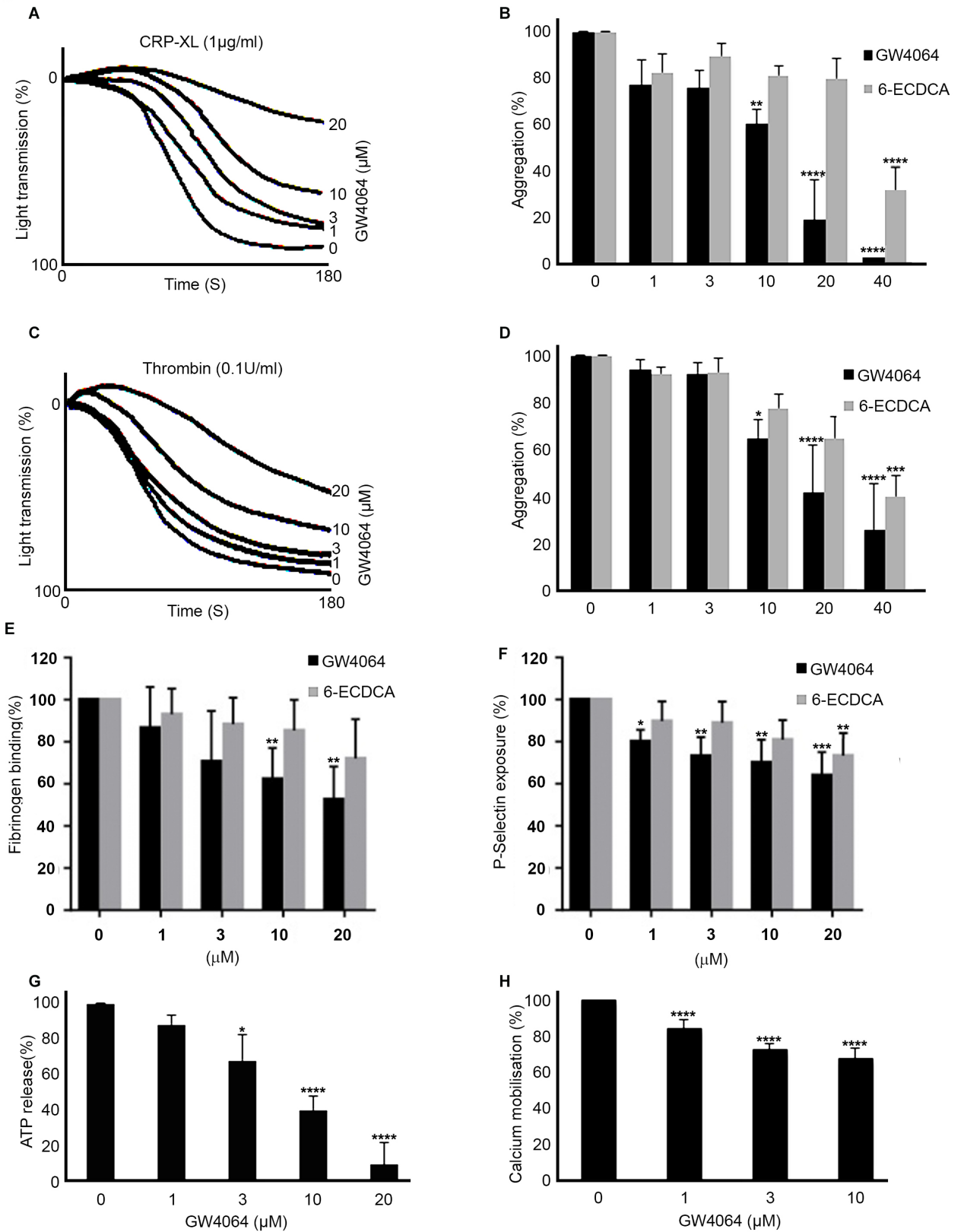


Figure 2 - FXR ligands inhibit platelet activation. Washed human platelets were treated for 5 min with increasing concentrations of FXR ligands, GW4064, 6-ECDCA or vehicle

containing (DMSO (0.1% (v/v)), prior to stimulation for 180s with collagen-related peptide CRP-XL (1 $\mu\text{g mL}^{-1}$) or Thrombin (0.1 U/mL) and aggregation measured at 37°C under constant stirring conditions (A-D). The effect of GW4064 and 6-ECDC on fibrinogen binding and P-selectin exposure prior to stimulation with CRP-XL (1 $\mu\text{g mL}^{-1}$) were measured in human whole blood by Flow cytometry (E-F). Changes in ATP concentration released by washed platelets stimulated for 180s with CRP-XL (1 $\mu\text{g mL}^{-1}$) were used as a measure of dense-granule secretion and monitored simultaneously with aggregation in an optical lumi-aggregometer using a luciferase detection system (G). Calcium mobilization was assessed in Fura-2AM-loaded PRP pre-incubated with increasing concentration of GW4064 in the presence of EGTA to prevent influx of extracellular calcium and then stimulated with CRP-XL (1 $\mu\text{g mL}^{-1}$) (H). Numerical data represent the percentage compared with control, mean \pm SD (n=4). * $P \leq 0.05$, ** $P \leq 0.01$, *** $P \leq 0.005$, **** $P \leq 0.001$, (ANOVA with Bonferroni post test).

Figure 3

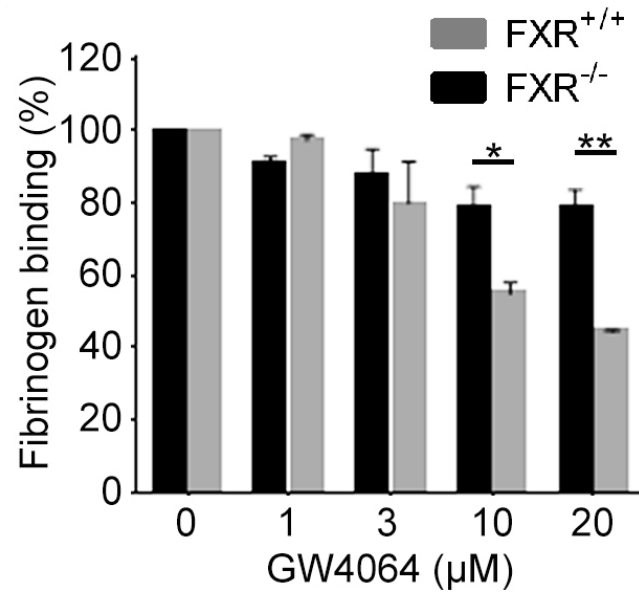


Figure 3 - The actions of GW4064 on platelets are mediated through FXR. Blood from FXR^{+/+} and FXR^{-/-} mice was treated with GW4064 or vehicle (containing DMSO 0.1% (v/v)) for 20 min prior stimulation with CRP-XL (1 μg mL⁻¹) and fibrinogen binding measured by flow cytometry. Data (median fluorescence intensity, expressed as a percentage of fibrinogen binding in the absence of GW4064) represent FXR^{-/-} mice platelets compared with FXR^{+/+} mice platelets (control), mean ± SD (n=4), **P* ≤ 0.05, ***P* ≤ 0.01 (*t*-test).

Figure 4

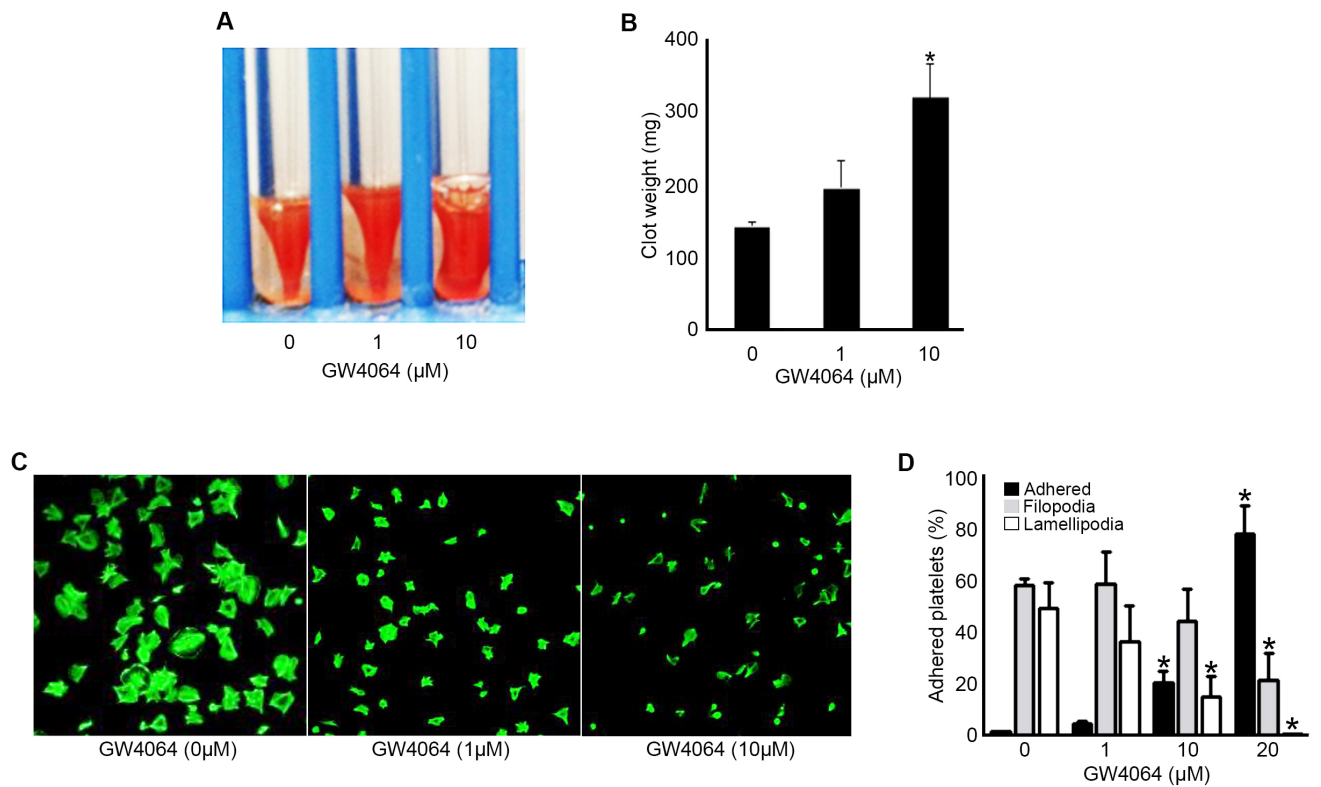


Figure 4 – GW4064 inhibits integrin $\alpha_{IIb}\beta_3$ -mediated outside-in signalling. Effect of GW4064 on clot retraction was analyzed *in vitro* (A-B). Representative images of clot retraction at 2h in the presence and absence of GW4064 (1, 10 μM), (A). GW4064 affects spreading in a concentration-dependent manner. Washed human platelets were allowed to spread for 45 min in the presence and absence of GW4064 (1 – 20 μM) on 100 $\mu\text{g mL}^{-1}$ fibrinogen-coated cover glasses and stained with Alexa fluor 488 labelled phalloidin prior to analysis by confocal microscopy (C). The images were analysed and the number of platelets found at different stages of platelet spreading were calculated (D). Numerical data represent the percentage compared with control, mean \pm S.E.M. (n=4). * $P \leq 0.05$, ANOVA with Bonferroni post test.

Figure 5

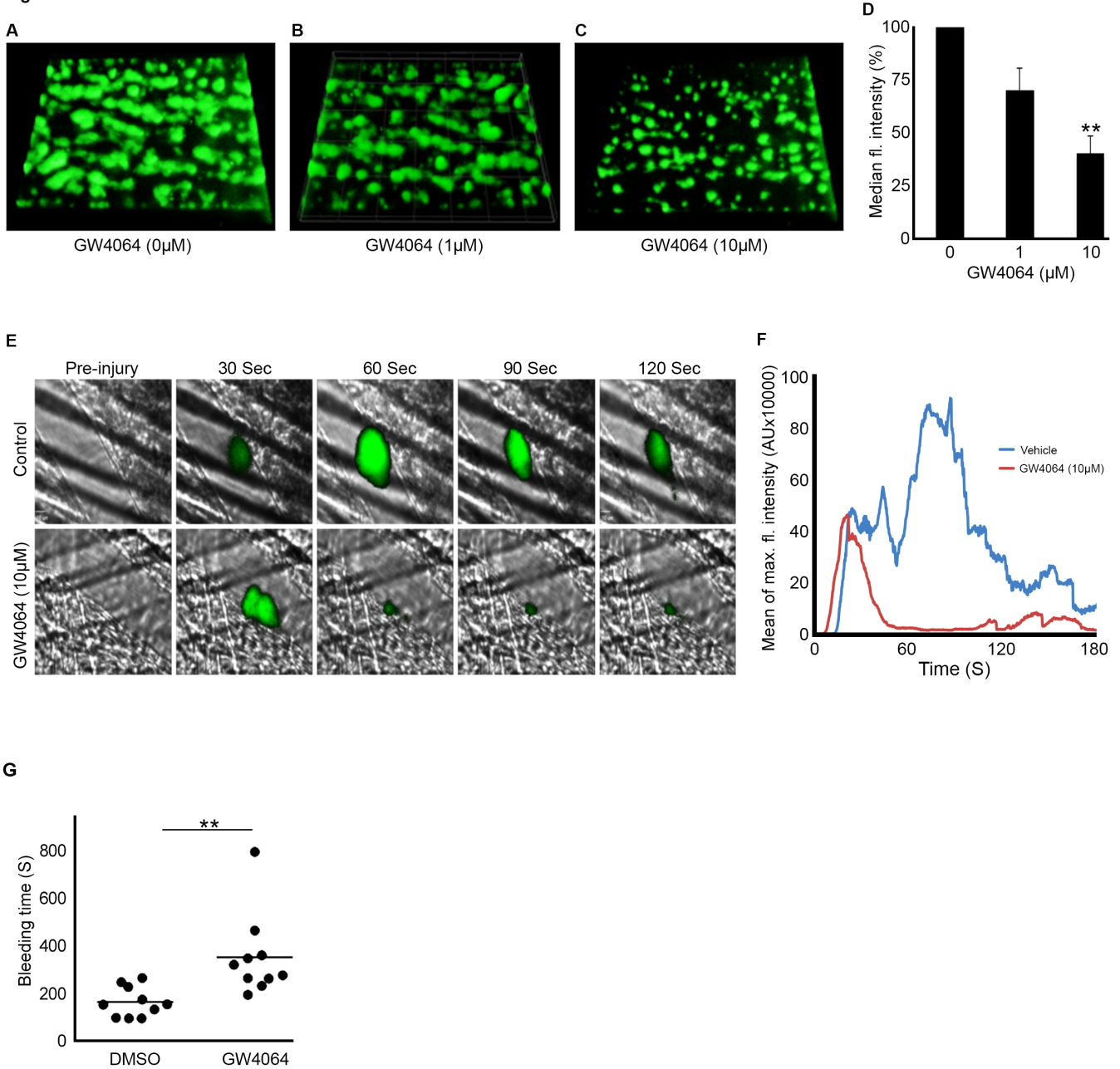


Figure 5 – GW4064 inhibits thrombus formation and hemostasis. Human whole blood labelled with the (DiOC₆)-lipophilic dye 3,3-dihexyloxacarbocyanine iodide was treated with vehicle (containing DMSO (0.1% (v/v)) (A) or GW4064 (1, 10 μ M) (B-C) for 5 min and perfused through collagen-coated (400 μ g mL⁻¹) Vena8Biochips at a shear rate of 20 dyn/cm². Thrombi were recorded at 10 min period through a series of images in the Z-plane through their full depth using a Nikon eclipse (TE2000-U) microscope, and thrombus fluorescence intensity was calculated using the Slidebook, version 5. The fluorescence intensity of thrombi obtained in the absence of GW4064 was taken as 100% (D). Cumulative data represent mean \pm SD (n=6), $P^* \leq 0.05$, $**P \leq 0.01$ (*t*-test). *In vivo* thrombosis was assayed using a laser

injury model by intravital microscopy. GW4064-estimated concentration (10 μ M) or vehicle (containing DMSO (0.1% (v/v))) was administered intravenously to mice, and platelets were fluorescently labeled by injection of Alexa 488-conjugated anti-GPIb antibody. After laser-induced injury of the cremaster muscle arterioles, accumulation of platelets was assessed. Representative images of thrombi obtained from mice treated with or without GW4064 at different time intervals are shown (E). Mean fluorescence intensity was measured from control and GW4064-treated mice ($n \geq 16$ thrombi from 4 GW4064-treated and 4 control mice) (F). The effect of GW4064 on hemostasis of mice was analyzed by measuring the bleeding time after tail tip excision. The bleeding time obtained with vehicle-treated group was compared with GW4064-treated mice (G). Data represent mean \pm SD ($n=10$ for each vehicle and mice-treated group), Statistical analysis was performed using the nonparametric Mann-Whitney test ($p=0.004$).

Figure 6

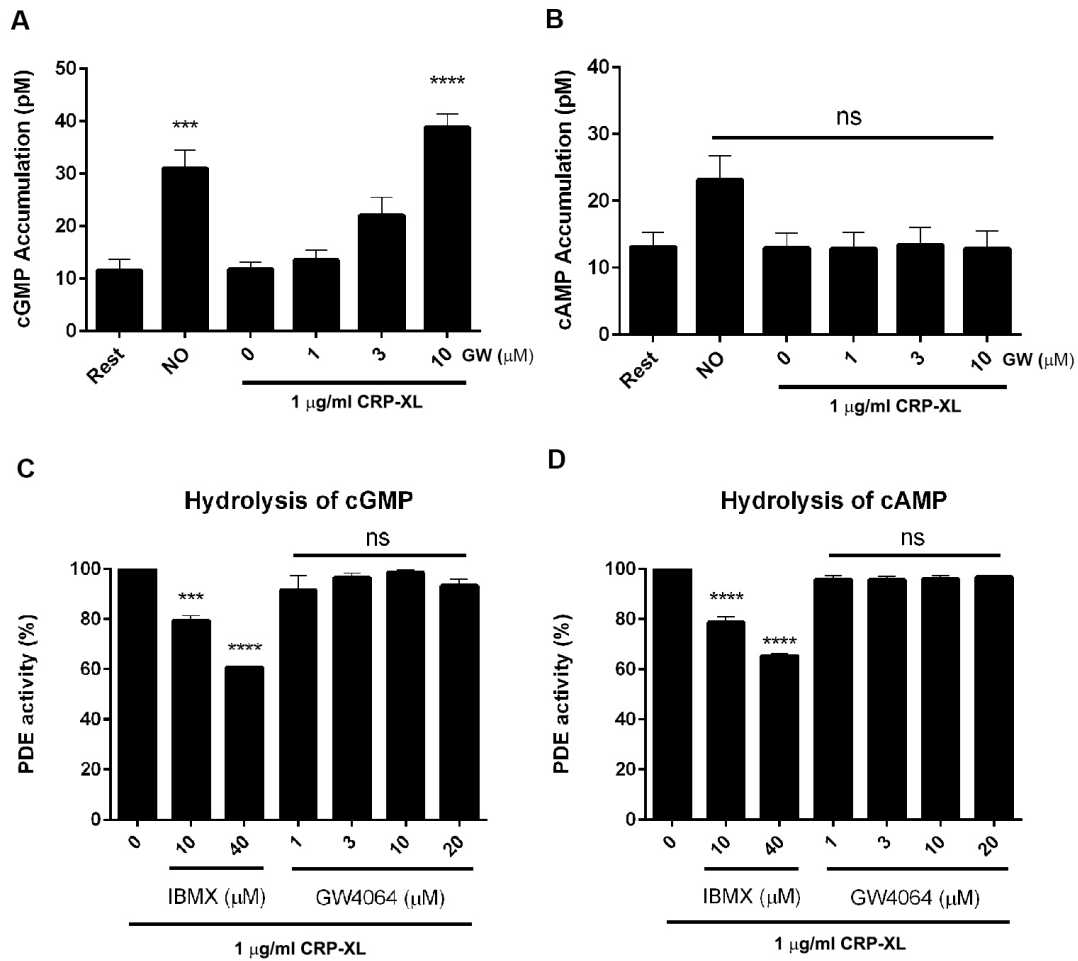


Figure 6 – GW4064 modulates platelet cyclic nucleotide signaling. The levels of cGMP (A) and cAMP (B) were measured in platelets on stimulation with CRP-XL ($1 \mu\text{g/ml}$) in the presence of GW4064 ($1\text{-}10 \mu\text{M}$) that was found to selectively increase cGMP levels. The effects of GW4064 ($1\text{-}10 \mu\text{M}$) on phosphodiesterase activity were measured on the hydrolysis of cGMP (C) and cAMP (D) to establish whether this corresponded to greater cyclic nucleotide production or hydrolysis. While the phosphodiesterase inhibitor IBMX inhibited cGMP and cAMP hydrolysis, GW4064 was without effect. The level of phosphodiesterase

activity obtained in the absence of GW4064 was taken as 100%. Data represent mean \pm SD (n=3), $P^{***} \leq 0.005$, $^{***}P \leq 0.001$, (ANOVA with Bonferroni post test).

Figure 7

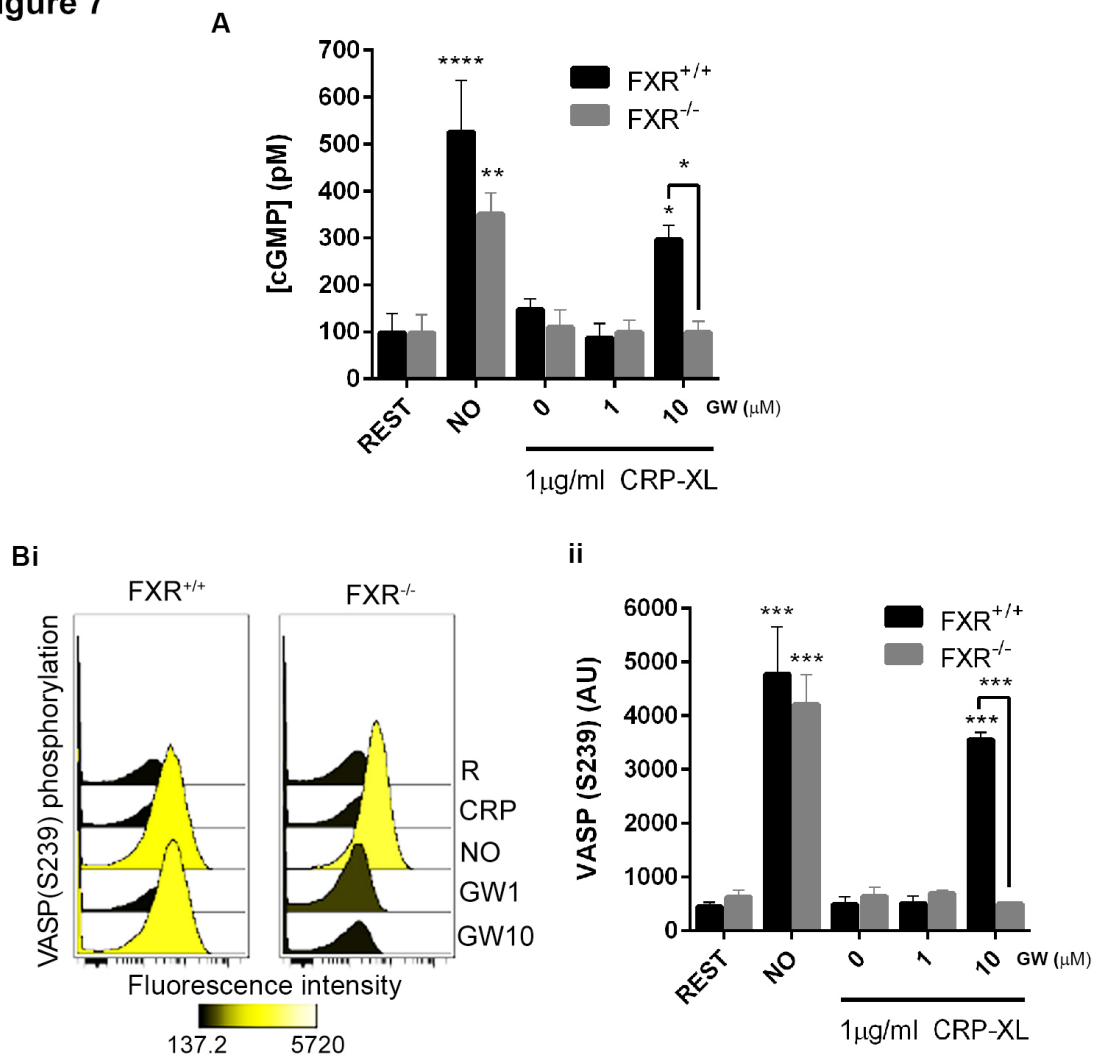


Figure 7 – Platelet FXR mediates cGMP signaling. Platelets derived from FXR^{+/+} and FXR^{-/-} mice were treated with GW4064 or vehicle containing (DMSO (0.1% (v/v))) for 20 min prior stimulation with CRP-XL (1 $\mu\text{g mL}^{-1}$). (A) cGMP levels were measured using the Enzyme immunoassay Biotrak (EIA) system and (B) VASP phosphorylation levels (S239) assessed by flow cytometry. R represents untreated resting platelet samples. Data represent FXR^{-/-} mice platelets compared with FXR^{+/+} mice platelets (control), mean \pm SD (n=4), * $P \leq 0.05$, ** $P \leq 0.01$, *** $P \leq 0.005$, **** $P \leq 0.001$ (ANOVA with Bonferroni post test).